AFRL-PR-WP-TR-2005-2021

HIGH-PERFORMANCE, SOFT MAGNETIC LAMINATES FOR AEROSPACE POWER SYSTEMS

Shiqiang (Sam) Liu

University of Dayton Research Institute
300 College Park
Dayton, OH 45469-0170

DECEMBER 2004

Final Report for 24 April 2000 – 24 October 2004

Approved for public release; distribution is unlimited.

STINFO FINAL REPORT

PROPULSION DIRECTORATE
AIR FORCE MATERIEL COMMAND
AIR FORCE RESEARCH LABORATORY
WRIGHT-PATTERSON AIR FORCE BASE, OH 45433-7251

NOTICE

Using Government drawings, specifications, or other data included in this document for any purpose other than Government procurement does not in any way obligate the U.S. Government. The fact that the Government formulated or supplied the drawings, specifications, or other data does not license the holder or any other person or corporation; or convey any rights or permission to manufacture, use, or sell any patented invention that may relate to them.

This report has been reviewed and is releasable to the National Technical Information Service (NTIS). It will be available to the general public, including foreign nationals.

This technical report has been reviewed and is approved for publication.

/s/
JOHN C. HORWATH
Electrical Engineer
Power Generation Branch

/s/
C. SCOTT RUBERTUS
Branch Chief
Power Generation Branch

/s/
CYNTHIA A. OBRINGER
Deputy Chief
Power Division
Propulsion Directorate

This report is published in the interest of scientific and technical information exchange and does not constitute approval or disapproval of its ideas or findings.

REPORT DOCUMENTATION PAGE

Form Approved
OMB No. 0704-0188

1. REPORT DATE *(DD-MM-YY)*	2. REPORT TYPE	3. DATES COVERED *(From - To)*
December 2004	Final	04/24/2000 – 10/24/2004

4. TITLE AND SUBTITLE
HIGH-PERFORMANCE, SOFT MAGNETIC LAMINATES FOR AEROSPACE POWER SYSTEMS

5a. CONTRACT NUMBER
F33615-00-C-2054

5b. GRANT NUMBER

5c. PROGRAM ELEMENT NUMBER
62203F

6. AUTHOR(S)
Shiqiang (Sam) Liu

5d. PROJECT NUMBER
3145

5e. TASK NUMBER
29

5f. WORK UNIT NUMBER
LQ

7. PERFORMING ORGANIZATION NAME(S) AND ADDRESS(ES)
University of Dayton Research Institute
300 College Park
Dayton, OH 45469-0170

8. PERFORMING ORGANIZATION REPORT NUMBER
UDR-TR-2004-00

9. SPONSORING/MONITORING AGENCY NAME(S) AND ADDRESS(ES)
Propulsion Directorate
Air Force Research Laboratory
Air Force Materiel Command
Wright-Patterson AFB, OH 45433-7251

10. SPONSORING/MONITORING AGENCY ACRONYM(S)
AFRL/PRPG

11. SPONSORING/MONITORING AGENCY REPORT NUMBER(S)
AFRL-PR-WP-TR-2005-2021

12. DISTRIBUTION/AVAILABILITY STATEMENT
Approved for public release; distribution is unlimited.

13. SUPPLEMENTARY NOTES
Report contains color.

14. ABSTRACT

Effort has been made to improve high-temperature (~600 °C) creep resistance of Fe-Co-V soft magnetic laminates for aerospace power system applications. An innovative approach has been applied to modify the commercial Hiperco 50 (Fe-Co-V) alloy sheets. This approach includes a small amount of cold deformation (with or slightly more than 3 percent) followed by an anneal at 850 °C for 3 hours. After the anneal, very large grains of a few hundred micrometers can be readily obtained. The grain size in the modified Fe-Co-V alloy sheets is at least 10 times as large as those in commercial Fe-Co-V alloys. Large grains were obtained in modified Hiperco 27, Hiperco 50A alloy sheets, as well.

The large-grain Fe-Co-V alloy sheets demonstrate significantly improved high-temperature creep resistance, especially the initial creep resistance, at 600 °C. The creep strains of the Fe-Co-V alloy with large grains are no more than 1/10 to 1/3 of those for the commercial alloys in the initial and middle periods of the test. In addition, Fe-Co-V alloy with large grains displays lower coercivity and higher permeability than the commercial Fe-Co-V alloy.

15. SUBJECT TERMS

16. SECURITY CLASSIFICATION OF:			17. LIMITATION OF ABSTRACT:	18. NUMBER OF PAGES	19a. NAME OF RESPONSIBLE PERSON (Monitor)
a. REPORT	b. ABSTRACT	c. THIS PAGE			John Horwath
Unclassified	Unclassified	Unclassified	SAR	42	19b. TELEPHONE NUMBER *(Include Area Code)* (937) 255-9190

Standard Form 298 (Rev. 8-98)
Prescribed by ANSI Std. Z39-18

TABLE OF CONTENTS

LIST OF FIGURES

LIST OF FIGURES (Concluded)

LIST OF TABLES

1. CONTRACT OBJECTIVE

The objective of this MEA PRDA effort was to determine the efficacy of implementing a low-deformation cold rolling and recrystallization process to produce high creep resistant Fe-Co alloys at high temperature with excellent soft magnetic properties. These alloys will be used in aerospace electrical systems, such as auxiliary power sources in aircraft. Fe-Co alloy materials that have improved creep resistance at 600°C, achieved by a substantial increase in grain size, were developed through a systematic study of the cold rolling/recrystallization parameters and their influence on high temperature creep behavior.

2. BACKGROUND

2.1 Requirement for High-Temperature Soft Magnetic Materials

New high temperature magnetic materials are enabling technologies for the development of new power components such as magnetic bearings, Integrated Power Units (IPU), and Internal Starter/Generators (IS/G) for aircraft main propulsion engines. There is also potential impact in the automotive industry, particularly electric vehicles.

As an example of the need for improved soft magnetic materials and their application to aerospace power systems, the United States Air Force (USAF) is currently developing several power generation devices and magnetic bearings as part of its More Electric Aircraft Initiative (MEA). These power generation devices and magnetic bearings require operation at elevated temperatures and stress levels never before required for such components. The systems being designed and evaluated in the MEA employ soft magnetic materials that require operation at temperatures approaching 550 to 600ºC, while rotating at speeds as high as 60,000 rpm. The designs generally call for rotors and stators to be made by stacking thin (0.006") laminates of

the soft magnet material in sheet form, electrically isolated from one another to reduce eddy-current losses. These speeds create hoop stresses approaching 85 ksi, far beyond the creep strengths of current materials at those temperatures.

The development of new soft magnetic materials for high temperature applications to the ≈600°C range presents the theoretical as well as the practical challenge of enhancing the high temperature mechanical performance without degrading the magnetic properties. In structural alloys the improvement in high temperature mechanical properties is achieved through a combination of alloying, processing, and grain morphology control. For soft magnetic materials, however, some of these options may lead to degradation in magnetic behavior, or to an unacceptable mechanical embrittlement.

2.2 Creep and Plastic Deformation

Plastic deformation in polycrystalline metals and alloys is a very complex topic in both theory and practice. Among all parameters that affect plastic deformation of metals and alloys, especially pure metals and single-phased alloys, the characteristics of grain boundaries have special significance. High temperature mechanical behavior is divided into three main categories: (a) short-term tensile strength, (b) long-term creep resistance, and (c) oxidation resistance. This research project focused on the improvement in long-term creep resistance at 600°C. We analyzed and summarized results of previous research as follows and formed the technical basis of our proposed research effort:

- The structure of high-angle grain boundaries resembles that of a super-cooled liquid. In other words, grain boundaries are amorphous in nature. This characteristic of grain boundaries greatly affects the mechanical properties of metals and alloys.

- The dominant mechanism for plastic deformation of metals and alloys at low temperatures is dislocation movement. Grain boundaries impede dislocation movement and increase the strength. Hence, grain boundaries are stronger than grain interiors at low temperatures.
- As temperature increases, the grain boundaries, like all other glassy materials, eventually become softened, and above this temperature, grain boundaries are weaker than grain interiors.
- For Fe-Co based alloys, 600°C represents a $\approx 0.5\ T_m$ condition, where T_m is the melting point (expressed in absolute temperature). A temperature of $\approx 0.4\ T_m$ represents the start of the dislocation (or power-law) creep regime. The 600°C temperature range is well into the Coble-creep regime and the majority of the creep deformation and damage are obtained from grain boundary sliding.
- Therefore, there is a transition temperature, T_{tr}, below which fine grain structure is beneficial for mechanical properties. Conversely, when the operating temperature is above T_{tr}, large grain structure is beneficial. As mentioned above, as a rule of the thumb, T_{tr} is $\approx 0.4\ T_m$.

2.3 Previous Approaches Improving Creep Resistance of Fe-Co Materials

2.3.1 Grain refinement

Small amounts of Nb and/or C were added to Fe-Co alloy to refine its grain structure to achieve higher mechanical strength with only a slight sacrifice in magnetic properties. However, metals and alloys with fine grains have better mechanical properties only when the temperature is lower than T_{tr}. The melting temperature of 50%Fe-50%Co alloy is 1480°C, leading to a T_{tr} for 50%Fe-50%Co of ≈430°C. The operating temperature for Fe-Co based

alloy in MEA applications is ≈600°C, far beyond its T_{tr}. Therefore, grain refinement is not appropriate for improving creep resistance of Fe-Co alloy at high temperatures.

2.3.2 Dispersion strengthening

Dispersed Al_2O_3 particles were proposed to be added to Fe-Co-V alloys to improve its creep resistance at high temperatures. Dispersed particles are certainly effective in improving mechanical strength by hindering dislocations and forcing them to climb and cross-slip. However, this approach is not an appropriate one to improve creep resistance at high temperatures ($>T_{tr}$). At temperatures above T_{tr}, grain boundary sliding is primarily responsible for creep. If dispersed particles are distributed mainly in grain interiors, the improvement of mechanical properties is more likely to happen at temperatures $<T_{tr}$, but not $>T_{tr}$. Also, dispersed particles will pin not only dislocations, but also domain walls. Therefore, in addition to reducing $4\pi M_s$ of Fe-Co alloy, the addition of dispersed particles will reduce permeability, while also increasing coercive force and hysteresis loss.

3. APPROACH OF THIS RESEARCH EFFORT

It is intrinsically difficult to improve mechanical properties of a material and to maintain or improve its soft magnetic properties at the same time. Usually, when a material is made mechanically harder, it becomes magnetically harder, as well. However, by employing a unique approach, we can significantly improve high temperature creep resistance of Fe-Co alloy and, at the same time, its magnetic properties (permeability, coercive force, and hysteresis loss) can be also improved.

The basic concept of our approach was to minimize the grain boundary slide at high temperatures ($>T_{tr}$) by significantly reducing the volume of grain boundaries in the Fe-Co

alloy. The weakness of the grain boundaries at high temperatures can be eliminated completely by using single crystal material. Single crystal form created by directional solidification approach has been applied to Nimonic alloys used for turbine blades. Making thin Fe-Co sheet in single crystal form is technically impractical. In addition, magneto-crystalline anisotropy of a single crystal sheet may create other problems. Our alternative approach was to make Fe-Co sheet with extraordinarily large grains.

In the commercial Fe-Co alloy sheet, the average grain size is about a few microns. By applying a very simple process, it is possible to increase the grain size of the Fe-Co alloy in a hundred micron range. Thus, the volume of grain boundaries can be significantly reduced. Therefore, the high temperature (≥430°C) creep resistance of Fe-Co alloy sheet can be significantly improved. In addition, because grain boundaries, like any other crystal defects, impede domain wall movement, reducing the volume of grain boundaries will increase permeability, reduce coercivity and hysteresis loss of the Fe-Co alloy. Therefore, this is an approach that simultaneously improves both mechanical and magnetic properties.

The unique characteristic of this approach is to utilize the critical cold deformation followed by normal recrystallization anneal to form extraordinarily large grains. The recrystallization of cold-worked metals and alloys is a nucleation and growth process. The driving force for this process comes from the stored energy of cold-work. The recrystallized grain size depends upon the amount of deformation given to the metal before annealing. Generally speaking, the recrystallized grain size is related to the ratio of (N/G) where N is the rate of nucleation and G is the rate of growth. The larger the (N/G), the finer the grain size will be.

The critical amount of cold work is the minimum amount of cold deformation that allows the metal to recrystallize. In the situation of critical deformation, the level of the stored energy of cold work is very low and N and (N/G) are also very low, resulting in very large grain size after annealing.

4. EXPERIMENTS AND RESULTS

4.1 Fe-Co-V Sheets Used in This Research Project

The compositions of Fe-Co and Fe-Co-V sheets used in this study are given in Table 1. Among them, Hiperco 50A was obtained directly from Carpenter Technology Corporation and other alloys were obtained from Dr. Richard Fingers of AFRL/PRP, WPAFB. All these Fe-Co or Fe-Co-V alloy sheets have thickness of 0.013".

Table 1. Compositions of Fe-Co Alloys Used in This Study

Alloy	Composition (wt%)								
	C	Mn	Si	Cr	Ni	Nb	V	Co	Fe
Hyperco 27	0.01	0.25	0.25	0.60	0.60	-	-	27	Bal
Hyperco 50	0.01	0.05	0.05	-	-	0.05	1.90	48.75	Bal
Hyperco 50A	0.004	0.05	0.05	-	-	-	2.00	48.75	Bal
Hyperco 50HS	0.01	0.05	0.05	-	-	0.30	1.90	48.75	Bal

4.2 Process Parameters

These alloy sheet specimens were degreased using acetone and, then, annealed in dry hydrogen at 850°C for 3 hours according to the parameters shown in Figure 1. After the anneal, the alloy sheet specimens were cold rolled using three different deformation rate as shown in Table 2.

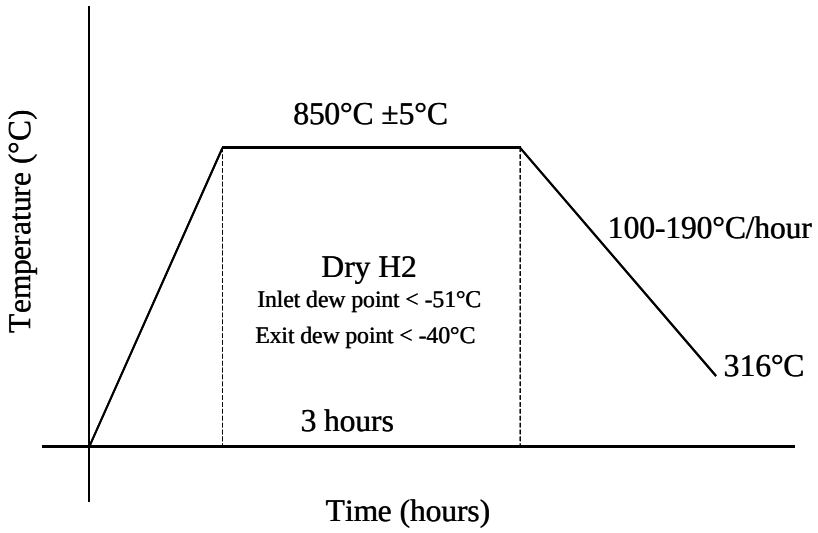

Figure 1. Annealing parameters before and after cold rolling.

Table 2. Cold Deformation Parameters

Specimen Set	Original Thickness (mil)	Final Thickness (mil)	Cold Deformation Rate (%)
1	6	5.7-5.8	3-5
2	6	5.9	1.6
3	6	5.6-5.7	5-6.7

The recrystallization anneal was performed after the cold rolling. The cold-rolled specimens were annealed at 850°C for 3 hours in a dry hydrogen atmosphere. The detailed parameters for the after-rolling anneal is also given in Figure 1.

4.3 Microstructures

4.3.1 Microstructures of commercial materials after annealing

As a comparison, the microstructures of the as-received commercial Fe-Co-V materials after annealing were observed using optic microscopy. The annealing parameters were the

same as those shown in Figure 1. Figures 2 through 4 show microstructures of commercial Hiperco 27, Hiperco 50, and Hiperco 50 HS, respectively.

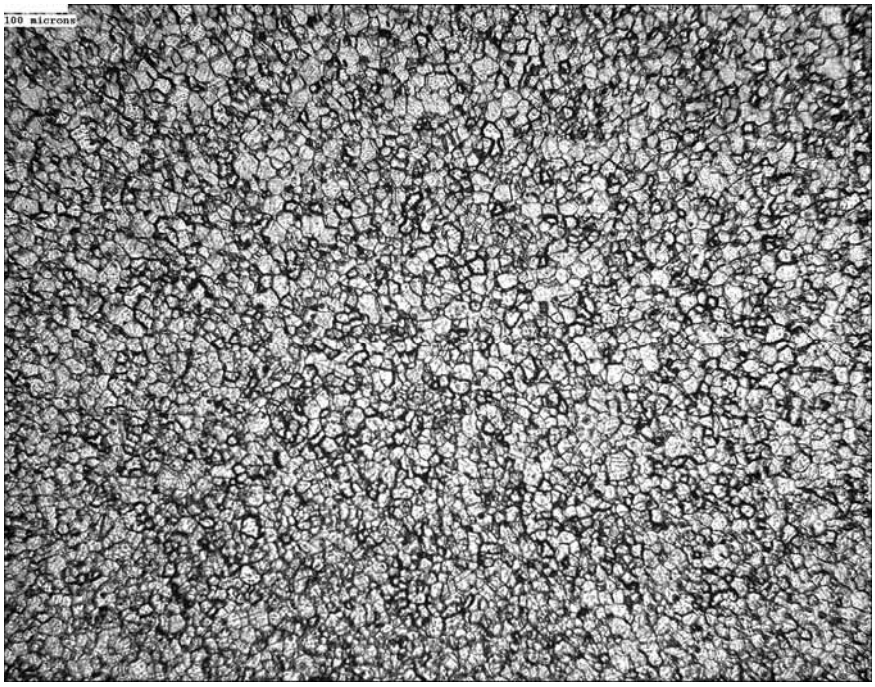

Figure 2. Microstructure of commercial Hiperco 27.

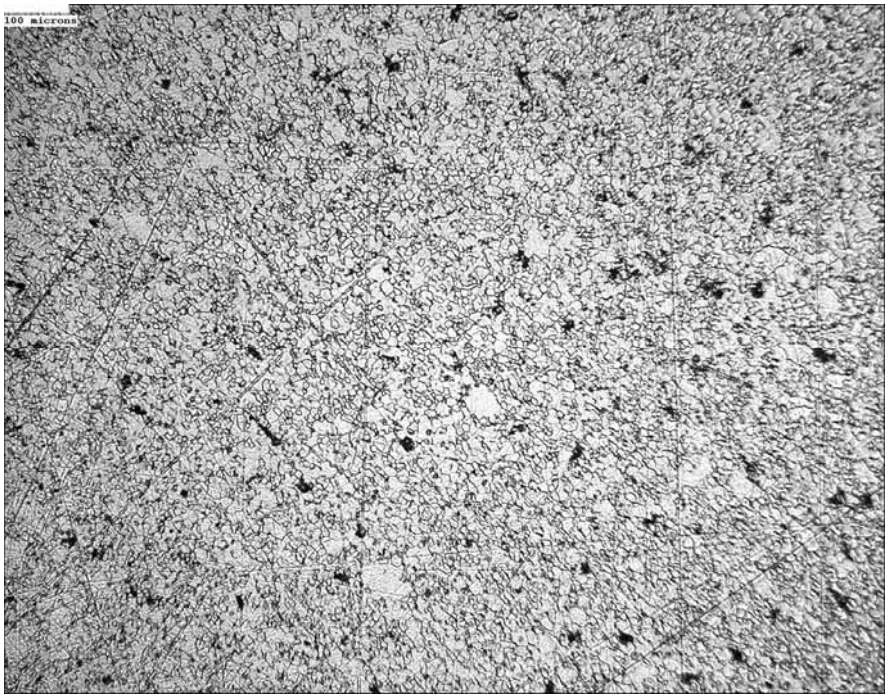

Figure 3. Microstructure of commercial Hiperco 50.

Figure 4. Microstructure of commercial Hiperco 50 HS.
(Please note that the scale bar is 10 micron for this micrograph.)

4.3.2 Microstructures of modified Fe-Co-V materials

The amount of cold deformation has strong effect on the grain size after the anneal. Very large grains can be obtained only when the cold deformation amount is 3% or slightly more than 3%. It is not easy to obtain large grains when the cold deformation amount is beyond this range.

Figure 5 shows microstructure of a modified Hiperco 50 specimen that was cold rolled with a deformation amount slightly smaller than 3% and annealed at 850°C for 3 hours. The grain size is only slightly larger than those of commercial Hiperco 50.

Figures 6 and 7 show microstructures of two modified Hiperco 50 specimens that were cold rolled with deformation amounts slightly more than 3% and exactly 3%, respectively, and after annealing at 850°C for 3 hours. In both cases, very large grains were obtained. Most grains are of a few hundred micrometers.

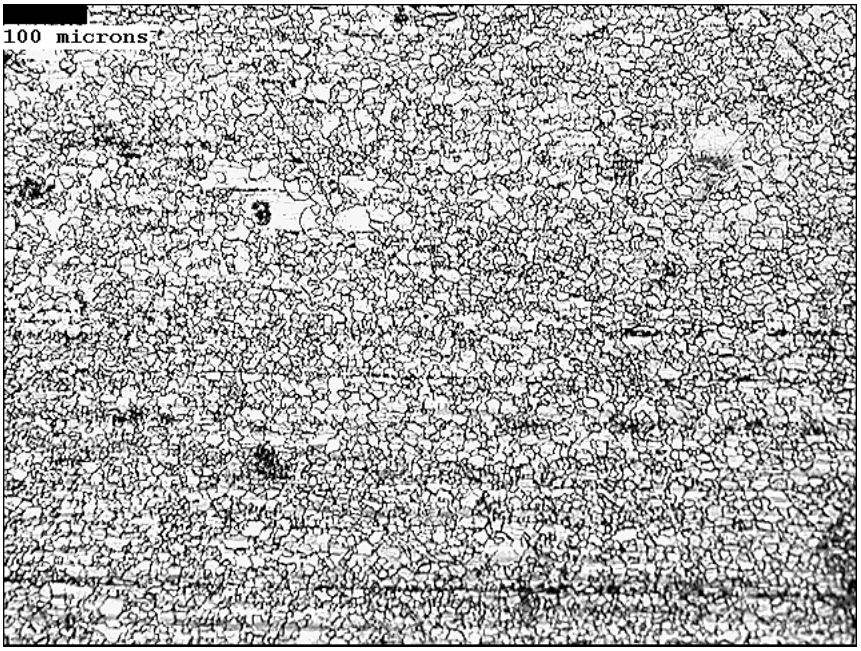

Figure 5. Microstructure of a modified Hiperco 50 specimen that was cold rolled with deformation slightly less than 3%.

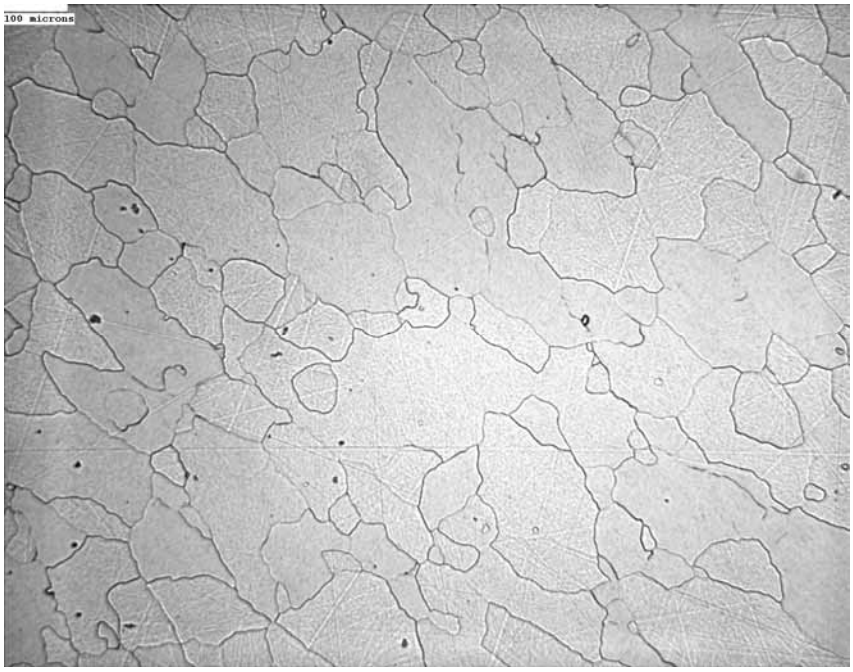

Figure 6. Microstructure of a modified Hiperco 50 specimen that was cold rolled with deformation slightly more than 3%.

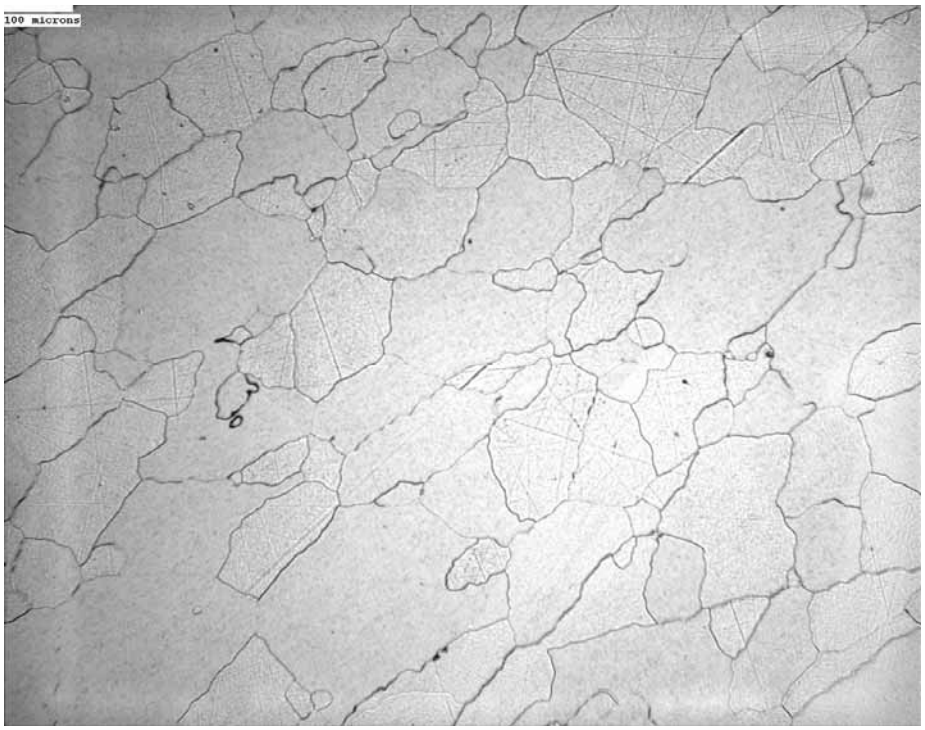

Figure 7. Microstructure of a modified Hiperco 50 specimen that was cold rolled with deformation equal to 3%.

Figures 8 and 9 show microstructures of modified Hiperco 50A and Hiperco 27, respectively. Very large grains were obtained in both specimens. Figure 10 shows microstructure of a modified Hiperco 50HS. Quite different from alloys mentioned above, cold rolling with 3% deformation and the subsequent annealing did not significantly change the grain size of the Hiperco 50HS alloy sheet. Apparently, the small additive of Nb in this alloy hindered the grain growth.

Sometimes, especially when the cold rolling amount was shift off the optimum deformation amount, non-uniform grain structure can be obtained. Figures 11 and 12 show microstructures of modified Hiperco 50 and Hiperco 50A specimens, respectively. In both cases, a mixture of large and small grains was obtained.

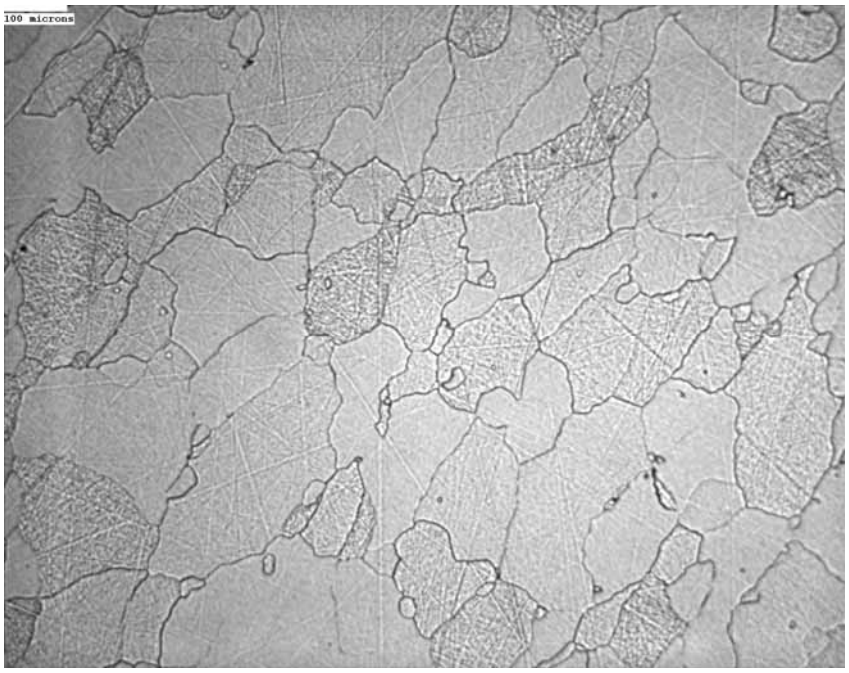

Figure 8. Microstructure of a modified Hiperco 50A specimen that was cold rolled with deformation slightly more than 3%.

Figure 9. Microstructure of a modified Hiperco 27 specimen that was cold rolled with deformation slightly more than 3%.

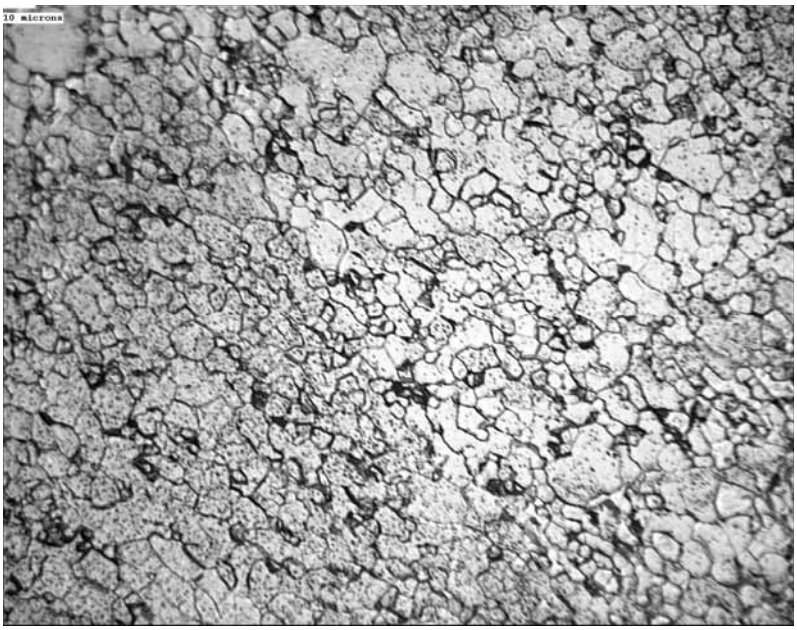

Figure 10. Microstructure of a modified Hiperco 50HS specimen that was cold rolled with deformation slightly more than 3%.

(Please note that the scale bar is 10 micron for this micrograph.).

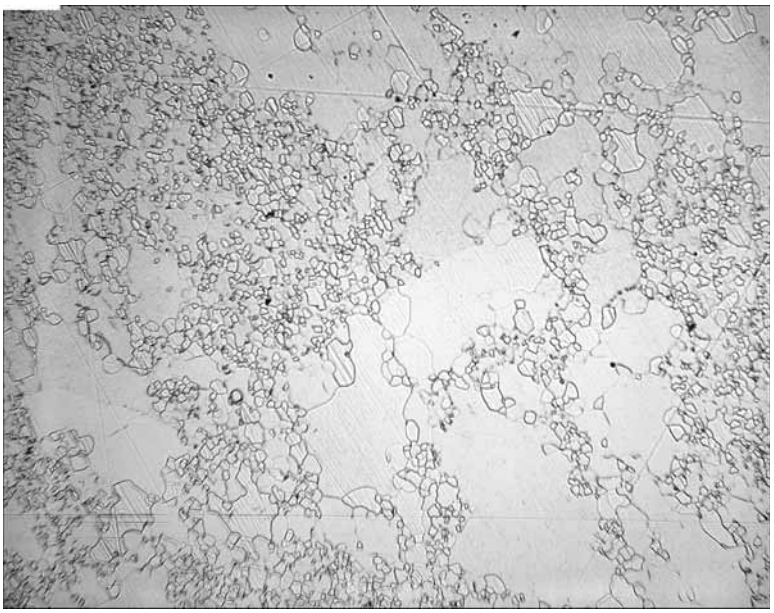

Figure 11. Microstructure of a modified Hiperco 50 specimen.

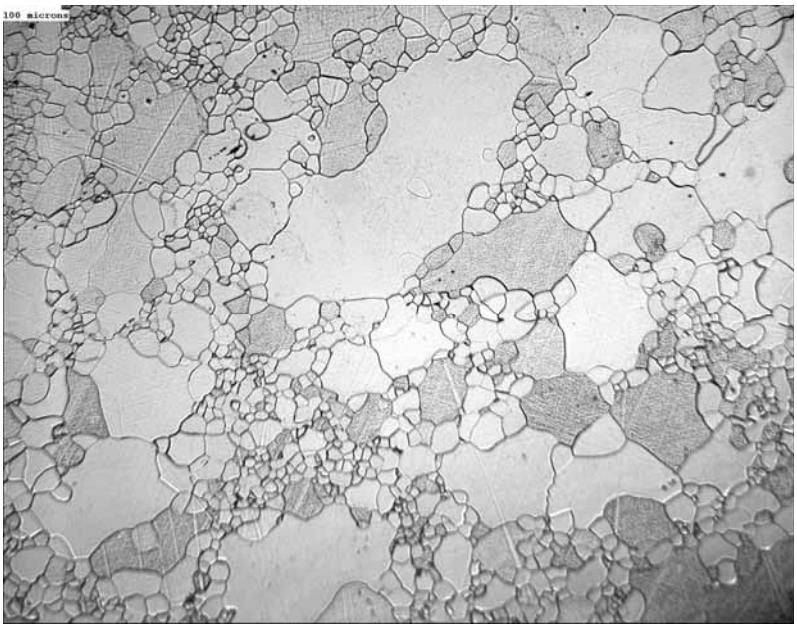

Figure 12. Microstructure of a modified Hiperco 50A specimen.

4.4 Creep Tests

4.4.1 Creep tests at 600°C

Creep tests at 600°C under 100 MPa, 120 MPa, or 150 MPa were performed for various commercial Fe-Co and modified Fe-Co alloy specimens. Figure 13 compares the creep strains of the commercial Hiperco 27 and modified Hiperco 27 with large grains. It can be seen from Figure 13 that the creep strain for both alloys are similar. The difference is that the large grain Hiperco 27 could be subjected to more creep strains before the specimen was broken.

Figure 14 compares the creep strains of a commercial Hiperco 50 and a modified Hiperco 50 with large grains tested at 600°C under 120 MPa. It can be seen from Figure 14 that in the beginning of the creep test, the creep strain for he commercial and large grain Fe-Co-V alloys are similar. After 250 hours, the large grain Fe-Co-V displays smaller creep strain than the commercial F-Co-V alloy. However, over time, the large grain Fe-Co-V displays an increased strain rate.

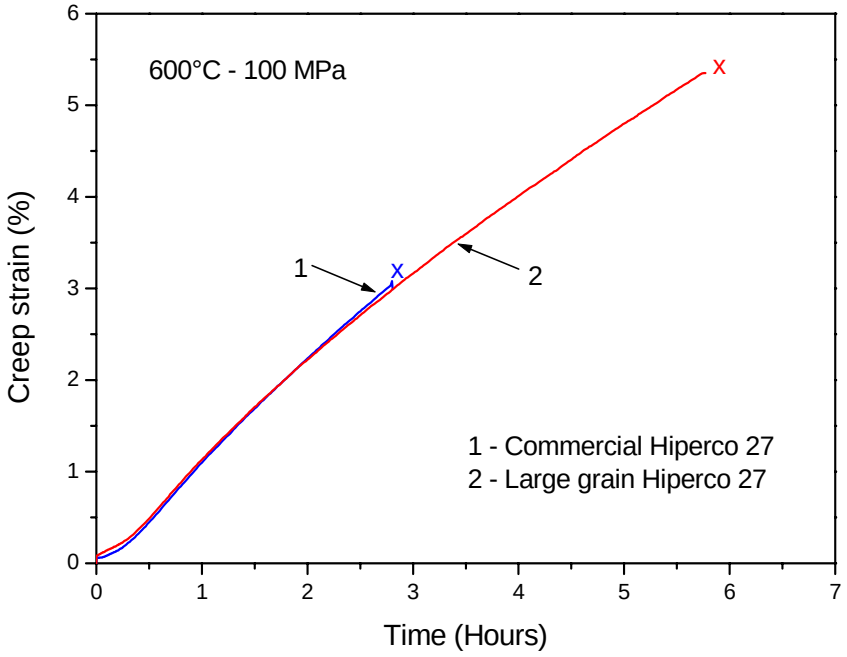

Figure 13. Creep strain vs. time for commercial Hiperco 27 and modified Hiperco 27 with large grains.

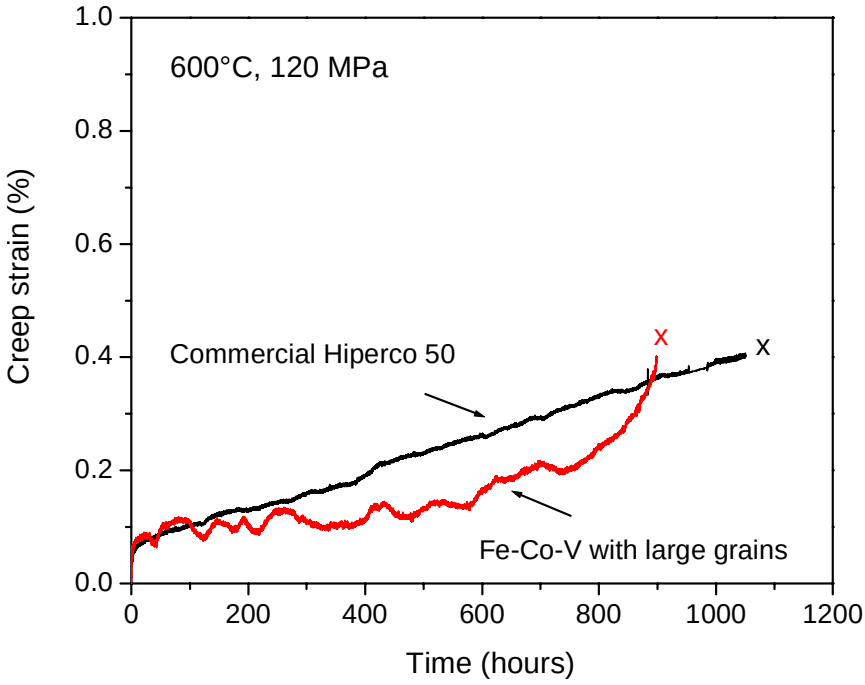

Figure 14. Creep strain versus time at 600°C and 120 MPa for commercial Hiperco 50 and modified Hiperco 50 with large grains.

Figure 15 shows creep strain versus time at 600°C under 150 MPa for a modified Hiperco 50A specimen with large grains. Apparently, the modified Hiperco 50A alloy demonstrates much more creep strain than the modified Hiperco 50 alloy.

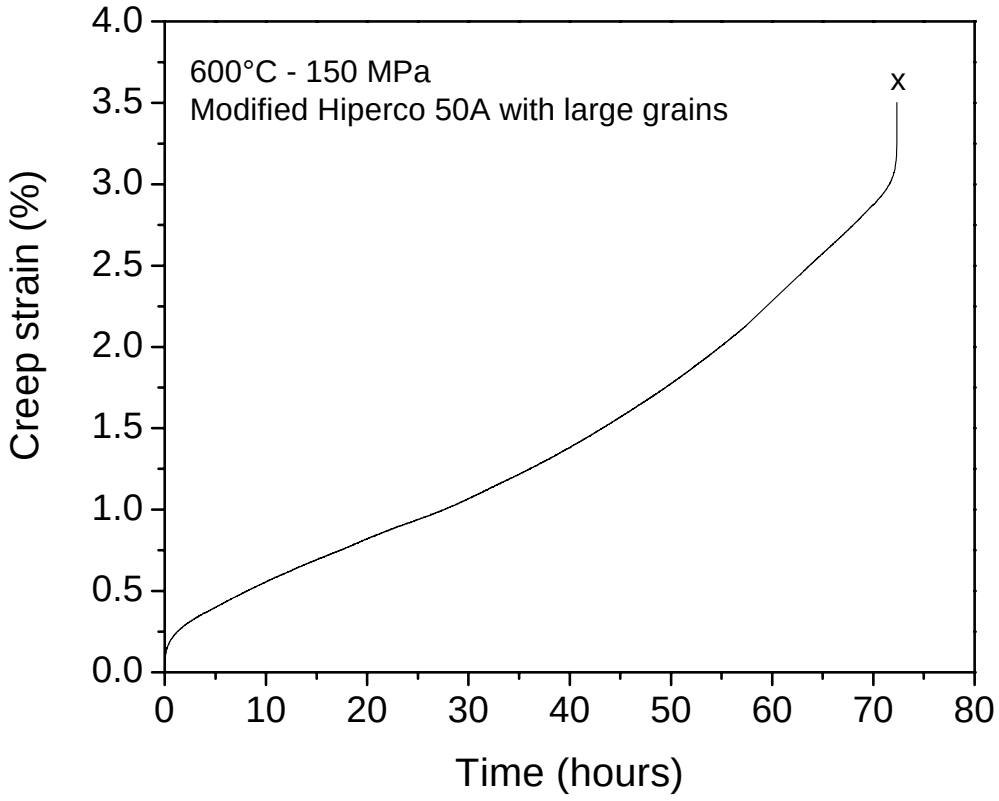

Figure 15. Creep strain versus time at 600°C and 150 MPa for a modified Hiperco 50A specimen with large grains.

Figure 16 shows creep stain versus time at 600°C under 150 MPa for a commercial Hiperco 50 and a modified Hiperco 50 with large grains. It can be seen that the modified large grain Hiperco 50 demonstrates much less initial creep than the commercial Hiperco 50. After about 200 hours, the strain rate of the modified Hiperco increased. Figure 17 compares the creep test results of commercial Hiperco 50, commercial Hiperco 50HS, and modified Hiperco 50 with large grains. Clearly, the small grain Hiperco 50HS shows the largest creep strain.

The Hiperco 50HS alloy was especially designed for improved mechanical strength (HS stands for high strength). As shown in Table 1, this alloy contains 0.30 wt% Nb for grain refinement. The fine grain Hiperco 50HS may have improved mechanical strength at room temperature and temperatures lower than 600°C, However, at 600°C and 150 MPa its creep strain was much greater than that of commercial Hiperco 50 and modified Hiperco 50.

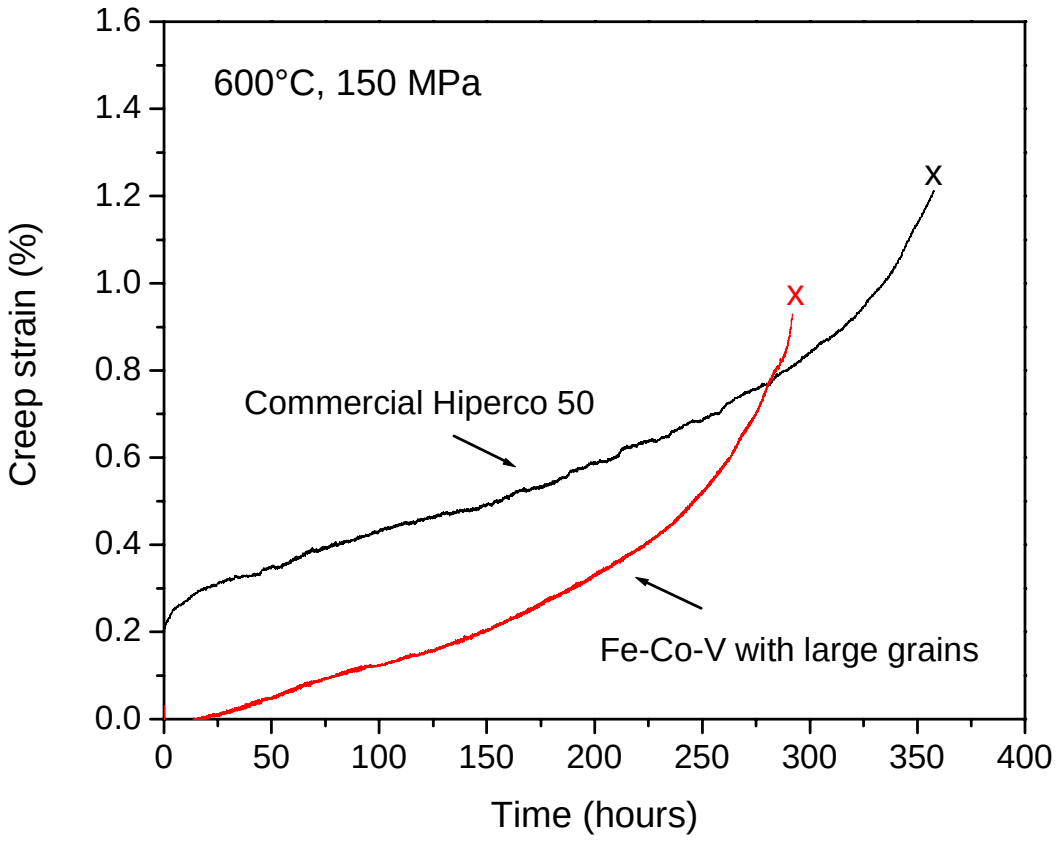

Figure 16. Creep strain versus time at 600°C and 150 MPa for commercial Hiperco 50 and modified Hiperco 50 with large grains.

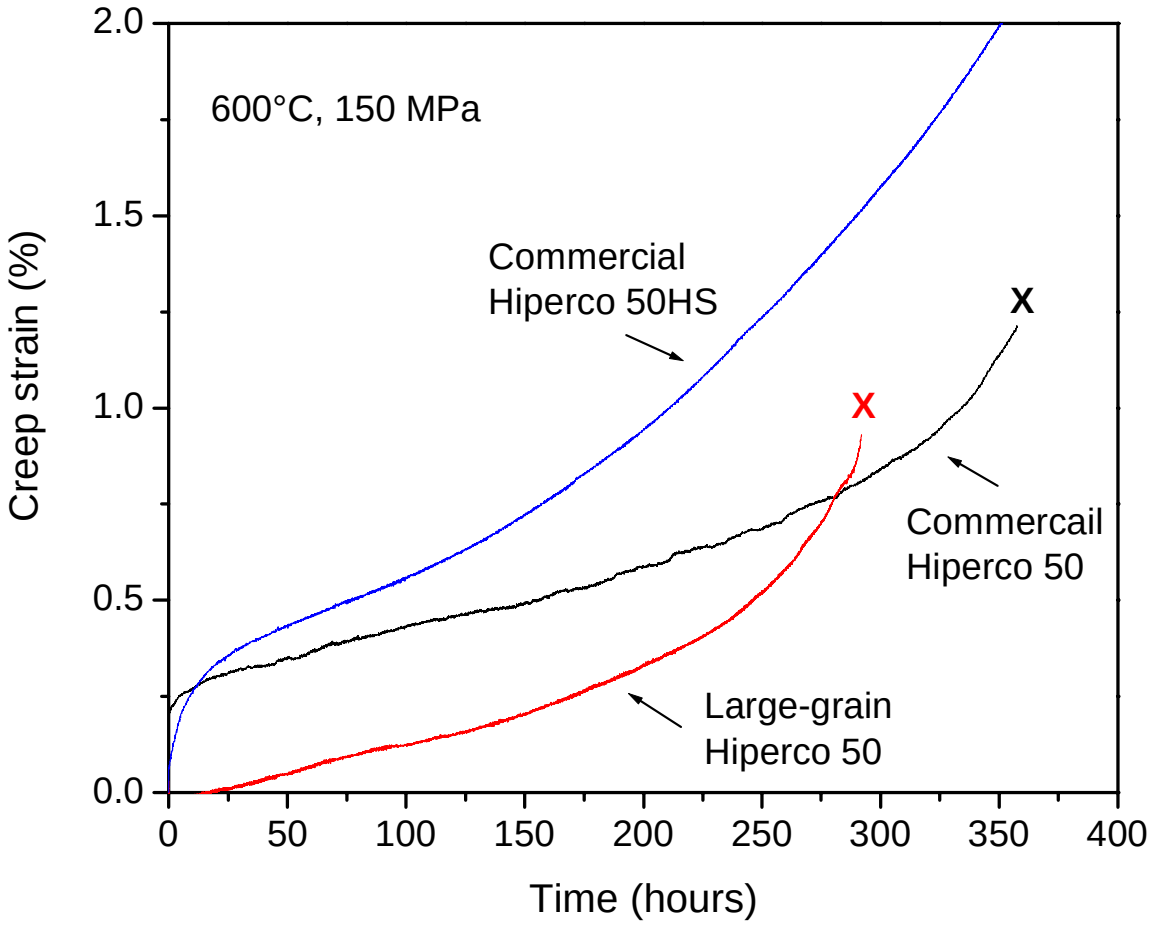

Figure 17. A comparison of creep strains of commercial Hiperco 50, Hiperco 50 HS, and modified Hiperco 50 with large grains.

Figure 18 summarizes the creep behavior at 600°C for various materials. The creep strain versus time for a composite Al_2O_3 coated Fe-Co material is also included in this figure. This composite material demonstrate a very low strain rate, indicating that a combination of low creep strain and low strain rate can be expected in ceramic/metal composite materials.

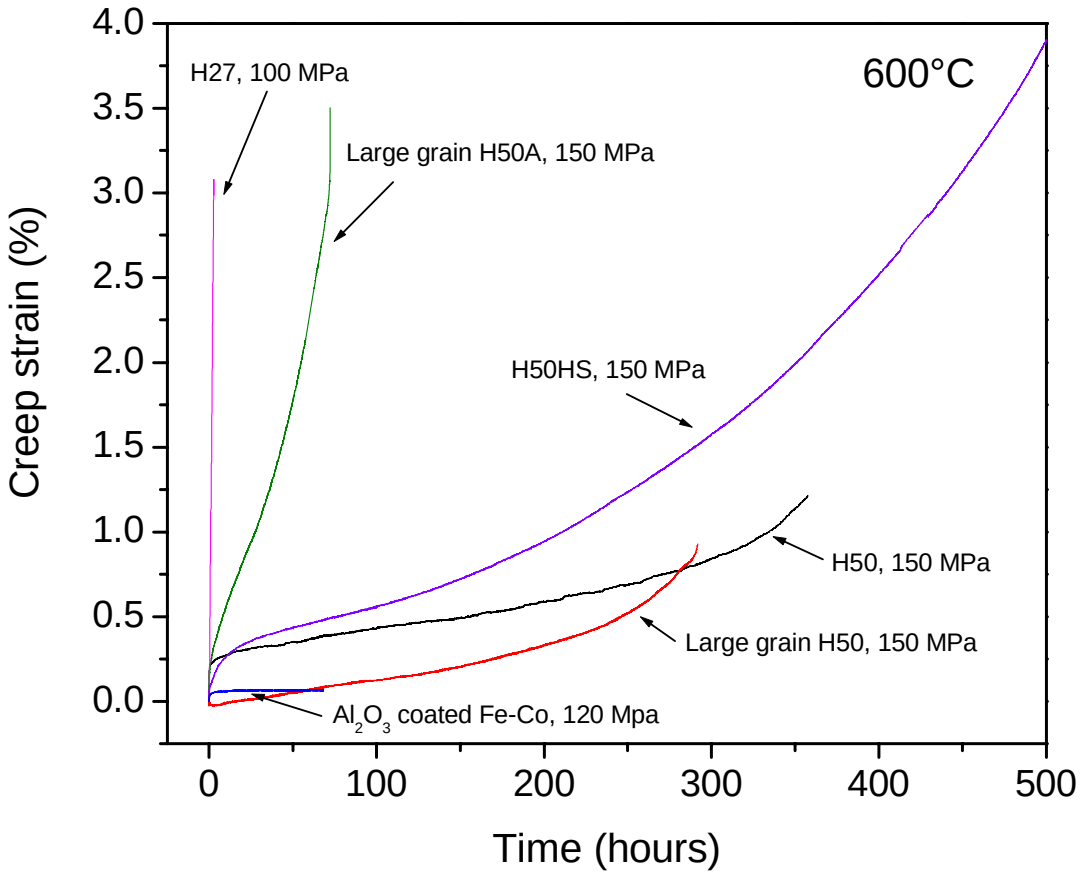

Figure 18. A summary of creep behavior tested at 600°C for various materials.

Figure 19 shows the creep strain versus time for another set of commercial and modified Hiperco 50 specimens tested at 600°C under 150 MPa. All modified Hiperco 50 with large grains show lower creep strain than their commercial counterpart. However, the commercial Hiperco 50 and some modified Hiperco 50 (specimens 2 through 4) demonstrate higher creep level as compared with the results shown in Figure 16.

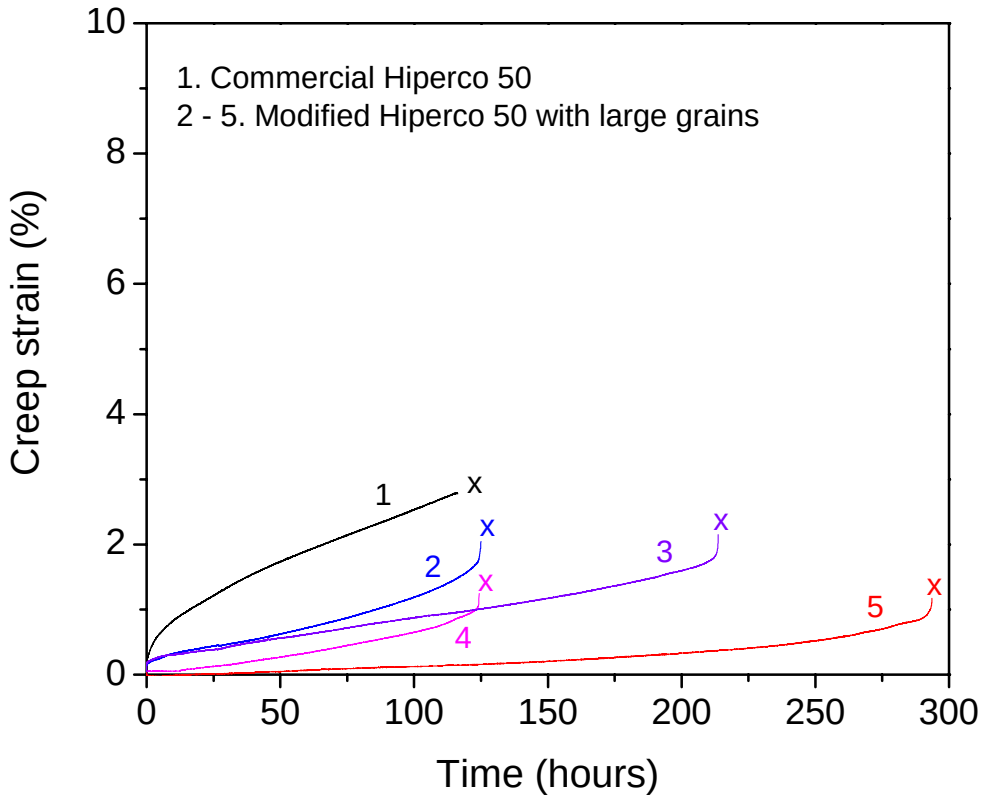

Figure 19. Creep strain vs. time for another set of commercial and modified Hiperco 50 specimens tested at 600°C under 150 MPa.

4.4.2 Creep tests at 550°C and 650°C

The creep test was also performed at 550°C and 650°C under 150 MPa for commercial Hiperco 50 and modified Hiperco 50 with large grains. Figure 20 shows the creep strain versus time for a commercial Hiperco 50 and a modified Hiperco 50 tested at 550°C under 150 MPa. This test shows that the modified Hiperco 50 has much more creep strain than the commercial Hiperco 50. Figure 21 shows the creep strain versus time for a commercial Hiperco 50 and a modified Hiperco 50 tested at 650°C under 150 MPa. In this case, the modified Hiperco 50 demonstrates slightly low creep strain than the commercial Hiperco 50.

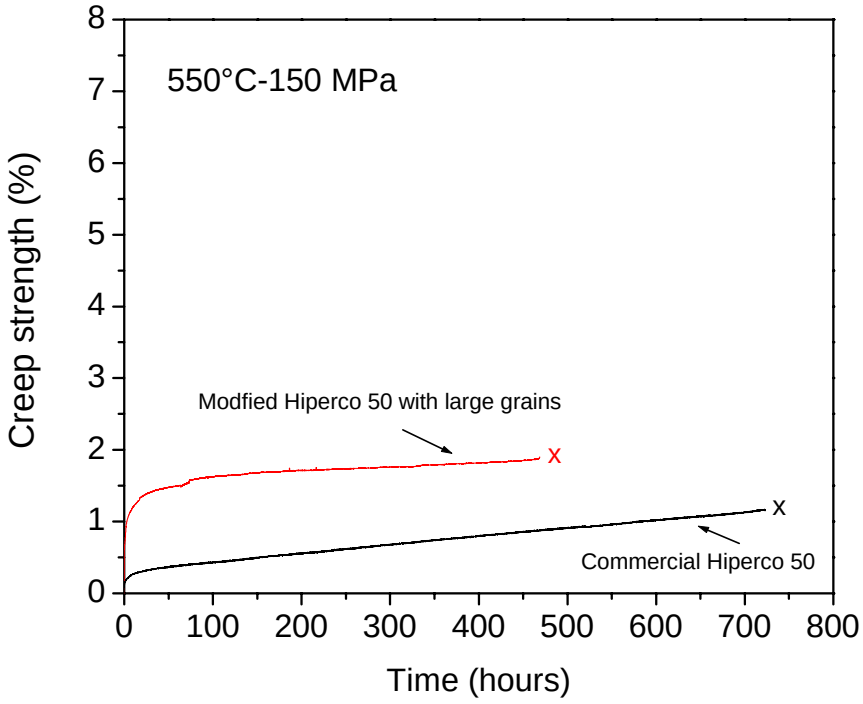

Figure 20. Creep vs. time for commercial Hiperco 50 and modified Hiperco 50 at 550°C under 150 MPa.

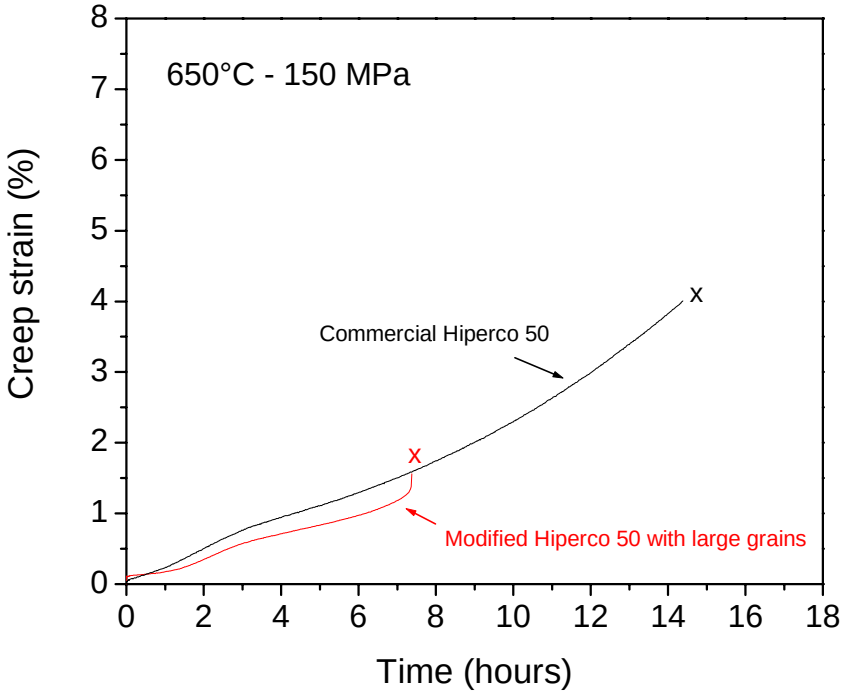

Figure 21. Creep vs. time for commercial Hiperco 50 and modified Hiperco 50 at 650°C under 150 MPa.

It seems that a transition temperature exists at a temperature lower than 600°C and higher than 550°C. Below this transition temperature, the small grain Fe-Co-V alloy has better creep resistance, while above this transition temperature, the large grain Fe-Co-V alloy shows better creep resistance. However, since only very limited number of specimens was tested at 550°C and 650°C, more experiments are need in order to more accurately define this transition temperature.

4.5 Magnetic Properties

4.5.1 DC magnetic properties

Ring specimens were cut from the commercial Hiperco 50 and the modified Hiperco 50 with large grains and, then, magnetic characterization was performed on the ring specimens. The DC magnetic measurements results are give as follows.

Figures 22 and 23 show DC hysteresis loops of modified Hiperco 50 with large grains and commercial Hiperco 50, respectively. It is obvious that the modified Hiperco 50 with large grains obtained in this research program has much better soft magnetic characteristics.

Figures 24 and 25 compare their permeability. It is very clear that the modified Hiperco 50 with large grains has much higher maximum permeability. Comparisons pf magnetic properties of these two types of materials are also given in Table 3.

Figures 26 through 28 show saturation induction, remanence, coercivity, and permeability of another set of modified Hiperco 50 specimens, respectively.

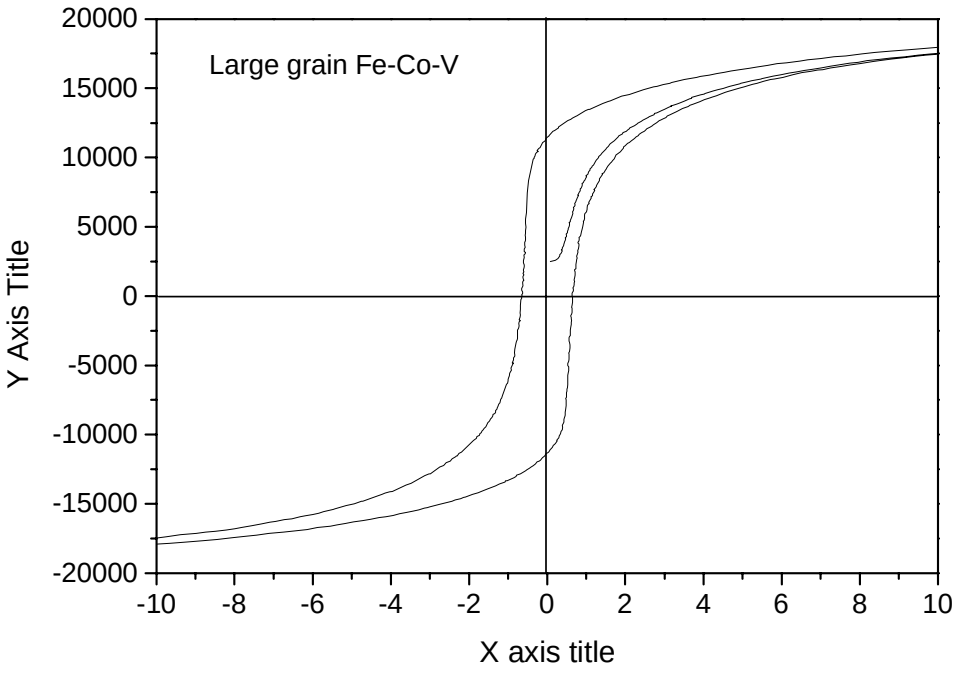

Figure 22. Hysteresis loop of modified Hiperco 50 with large grains.

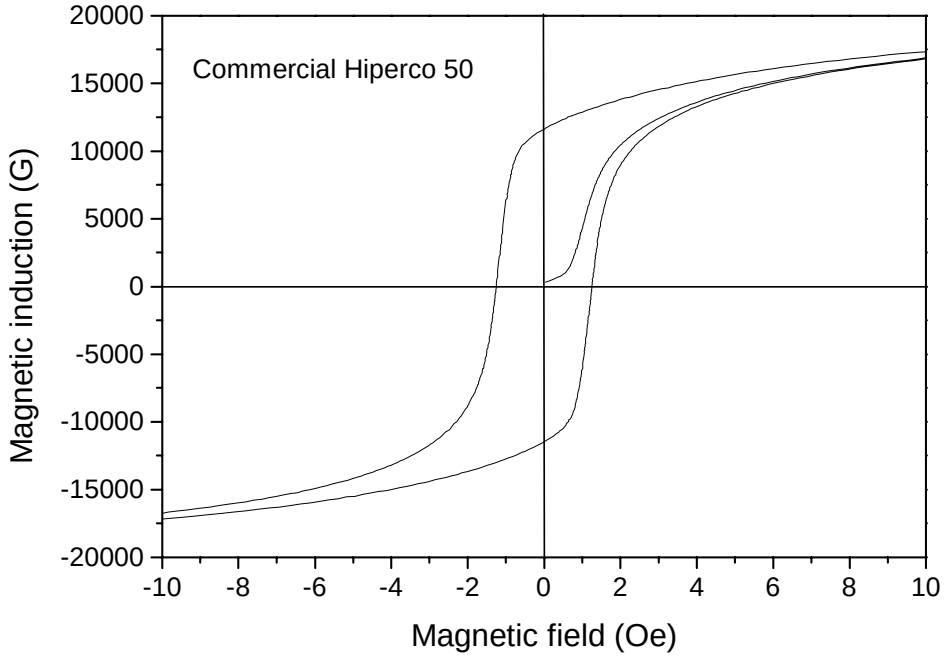

Figure 23. Hysteresis loop of commercial Hiperco 50.

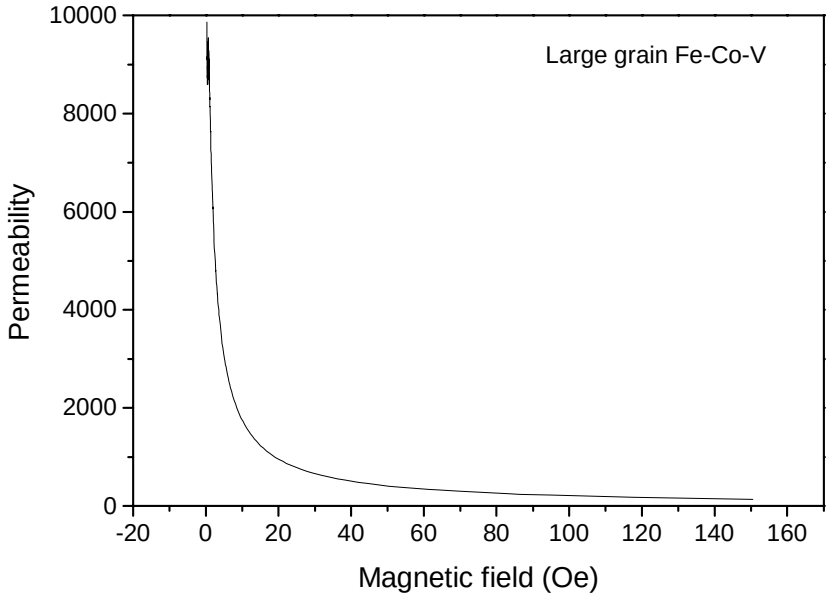

Figure 24. Permeability of Fe-Co-V alloy with large grains.

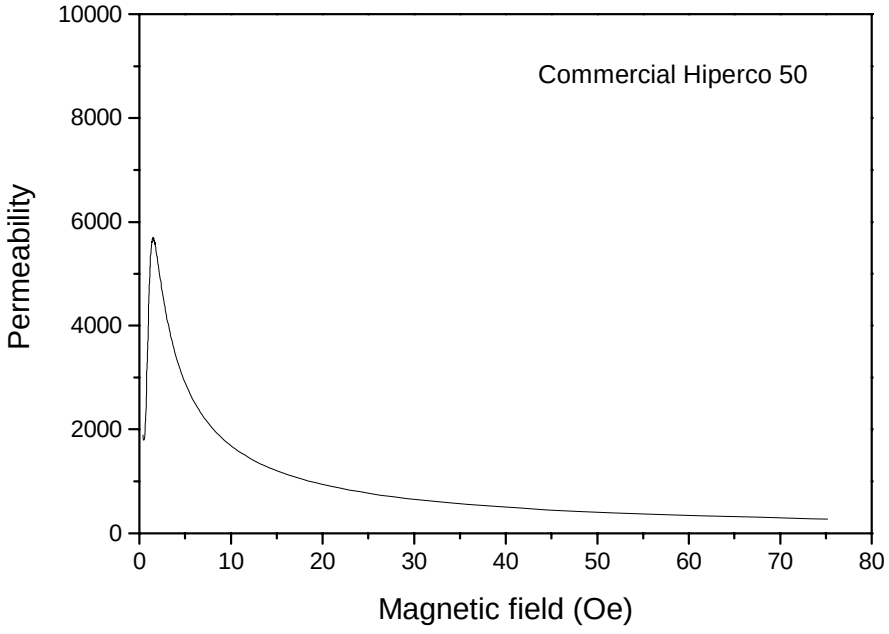

Figure 25. Permeability of commercial Hiperco 50 alloy.

Table 3. DC Magnetic Properties of Fe-Co-V Alloy with Large Grains and Commercial Hiperco 50

Material	Coercivity, H_c (Oe)	Maximum Permeability, μ
Fe-Co-V with Large Grains	0.639	9547
Commercial Hiperco 50	1.255	5607

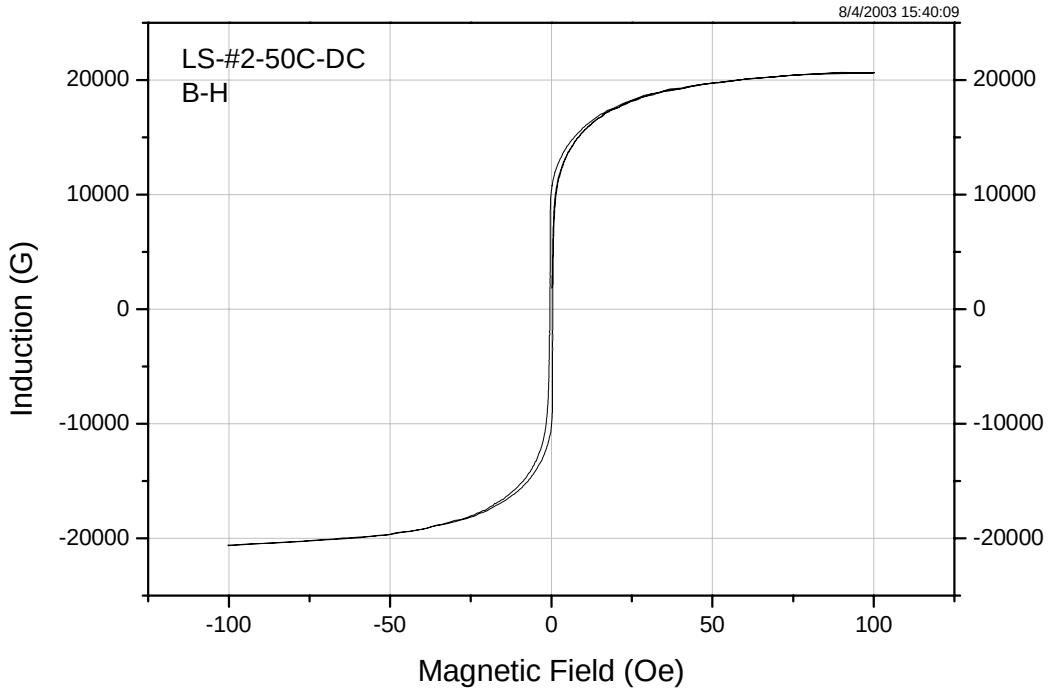

Figure 26. Hysteresis loop of a modified Hiperco 50 specimen showing saturation induction.

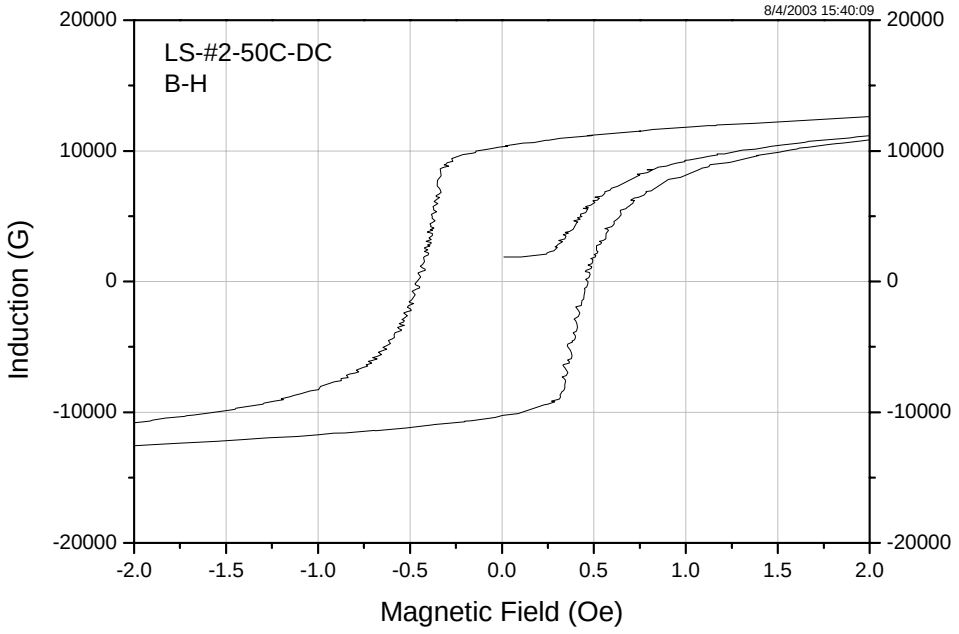

Figure 27. Hysteresis loop of the modified Hiperco 50 specimen showing remanence and coercivity.

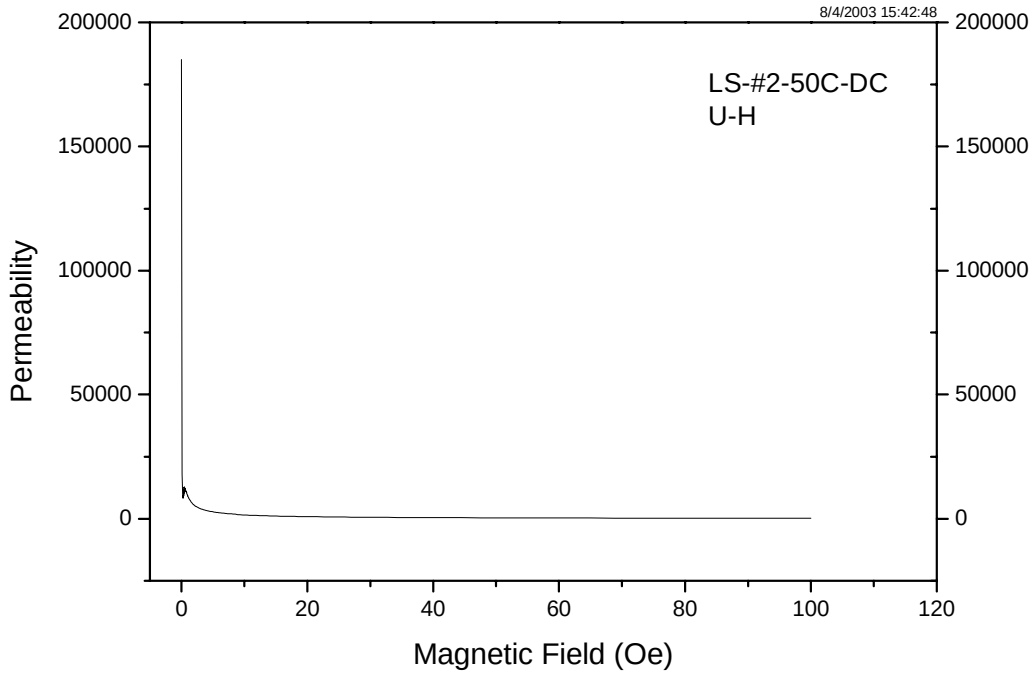

Figure 28. Permeability of the modified Hiperco 50 specimen.

Figures 29 through 31 show saturation induction, remanence, coercivity, and permeability of commercial Hiperco 50, respectively.

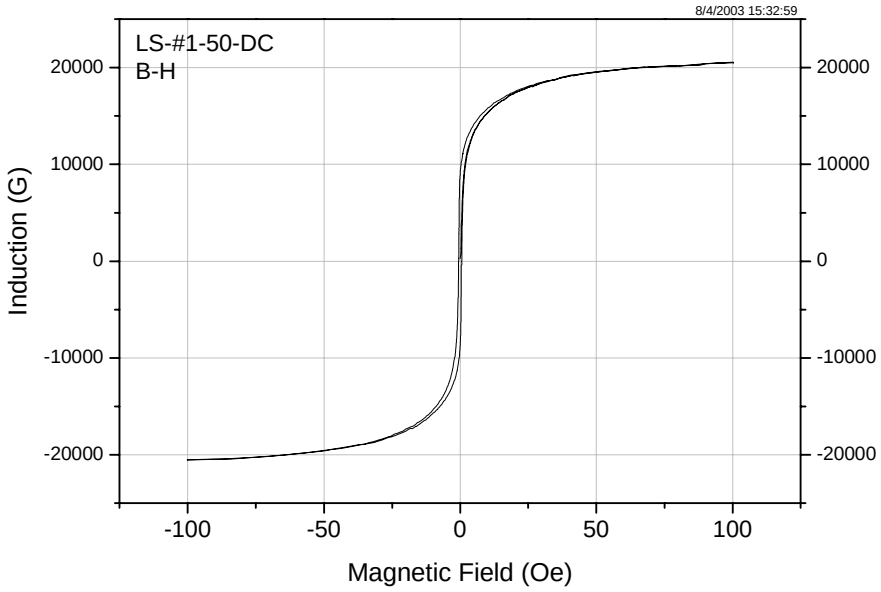

Figure 29. Hysteresis loop of a commercial Hiperco 50 specimen showing saturation induction.

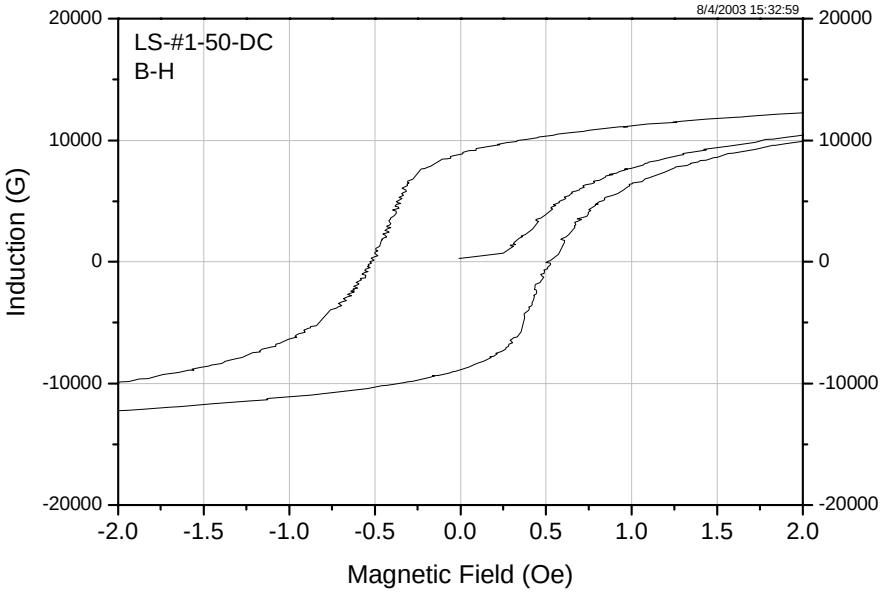

Figure 30. Hysteresis loop of the commercial Hiperco 50 specimen showing remanence and coercivity.

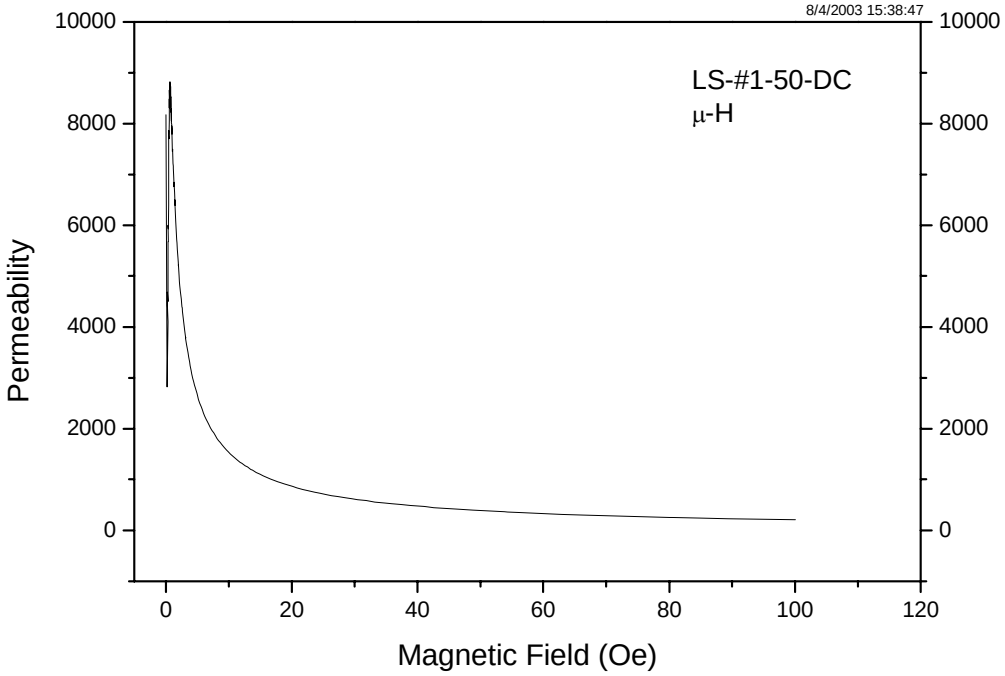

Figure 31. Permeability of commercial Hiperco 50 specimen.

Table 4 compares magnetic properties of commercial Hiperco 50 and modified Hiperco 50 with relatively large grains. Apparently, the modified material demonstrates higher induction at 100 Oe, higher remanence, lower coercivity, especially higher permeability. Because grain boundaries serve as a resistance to domain wall motion, these experimental results are easy understood.

Table 4. Magnetic Properties of Commercial Hiperco 50 and Modified Hiperco 50

	B at 100 Oe (G)	B_r (G)	H_c (Oe)	μ
Modified Hiperco 50	20,644	10,290	0.46	185,072
Commercial Hiperco 50	20,555	8,880	0.53	8,177

4.5.2 AC magnetic properties

Ring specimens were cut from the modified Hiperco 50 specimens with large grains. AC magnetic characterizations were performed on these specimens. Figures 32 and 33 show magnetization curves and permeability at various frequencies, respectively. These magnetic properties are similar as compared with commercial Hiperco 50 alloy.

Figure 34 shows the core losses of modified Hiperco 50 and commercial Hiperco 50 at 50, 100, 200, and 300 Hz. At these frequencies, the commercial Hiperco 50 demonstrates slightly lower core losses (lower curve for each frequency.). Figure 35 shows the core losses of modified Hiperco 50 and commercial Hiperco 50 at 400, 500, 700, and 1 kHz. At these frequencies, the modified Hiperco 50 shows slightly lower core losses (lower curve for each frequency.) Finally, Figure 36 shows the core losses of modified Hiperco 50 and commercial Hiperco 50 at 1.5, 2, and 3 kHz.

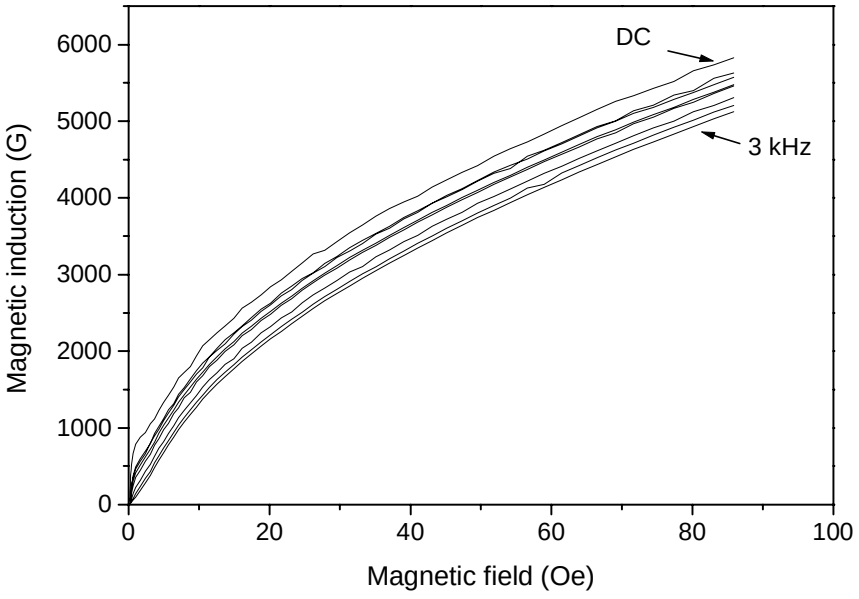

Figure 32. Magnetization curves of modified Hiperco 50 at a DC magnetic field and at AC magnetic field with 50 Hz, 100 Hz, 200 Hz, 400 Hz, 1 kHz, 2kHz, and 3k Hz, respectively.

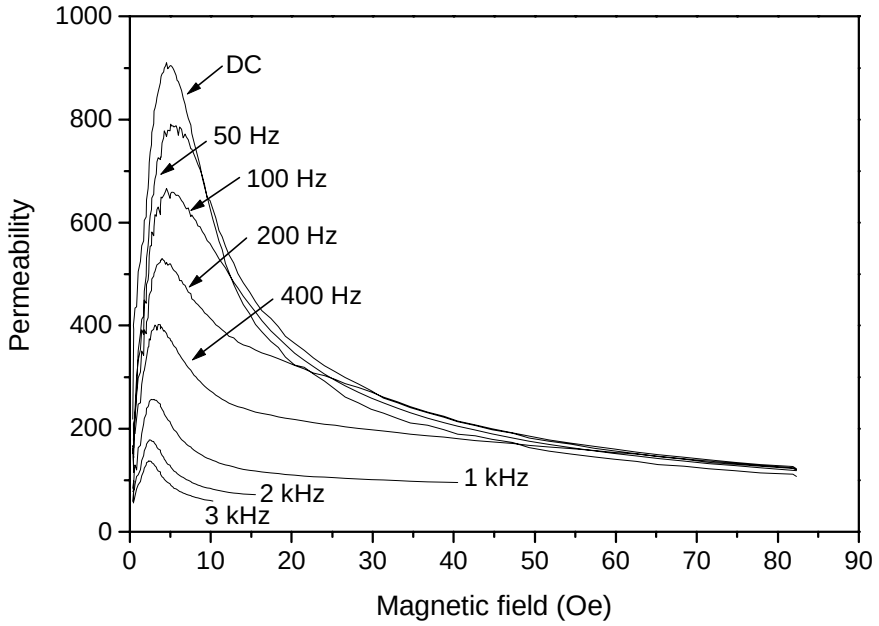

Figure 33. Core losses of modified Hiperco 50 and commercial Hiperco 50 at 50, 100, 200, and 300 Hz.

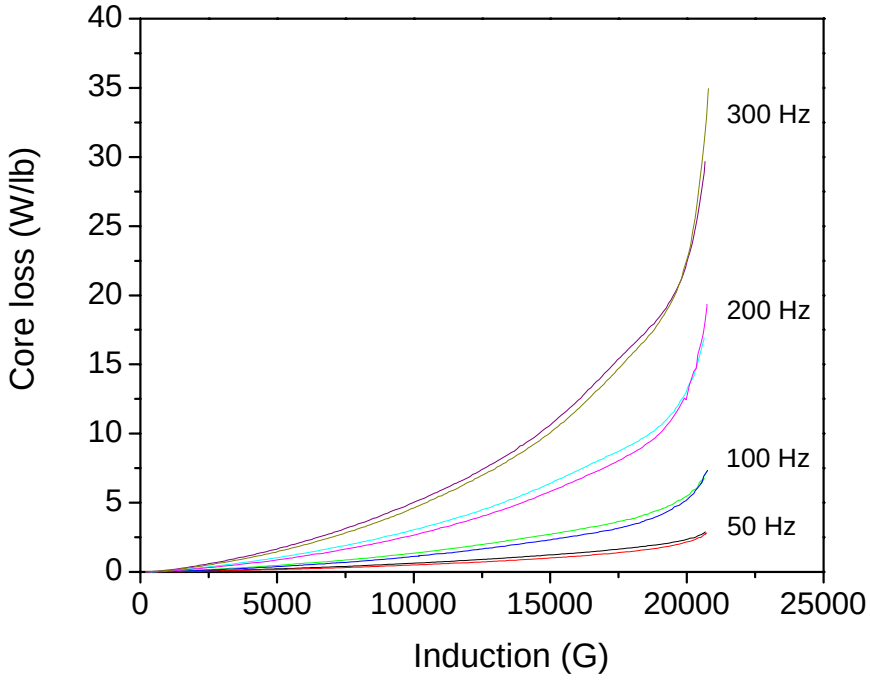

Figure 34. Core losses of modified Hiperco 50 and commercial Hiperco 50 at 50, 100, 200, and 300 Hz. For each frequency, the lower curve is for commercial Hiperco 50.

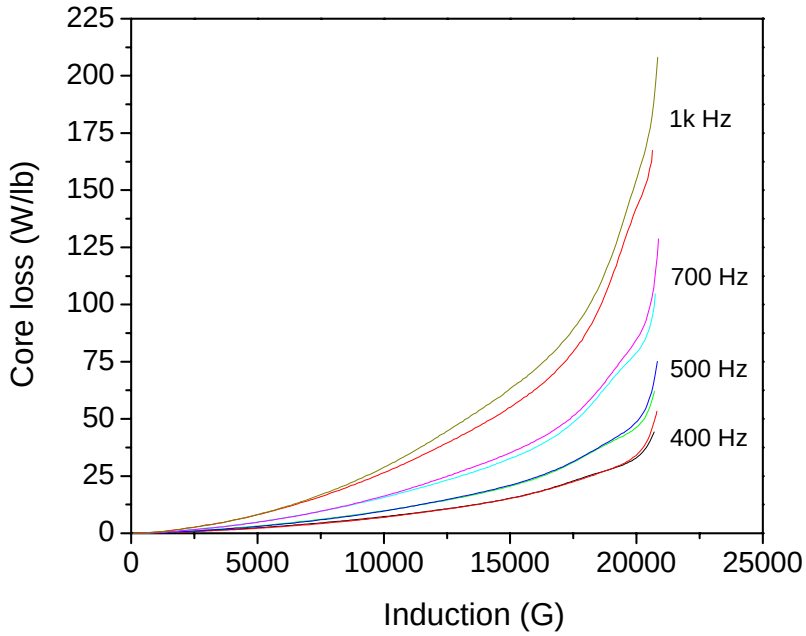

Figure 35. Core losses of modified Hiperco 50 and commercial Hiperco 50 at 400, 500, 700, and 1 kHz. For each frequency, the lower curve is for modified Hiperco 50.

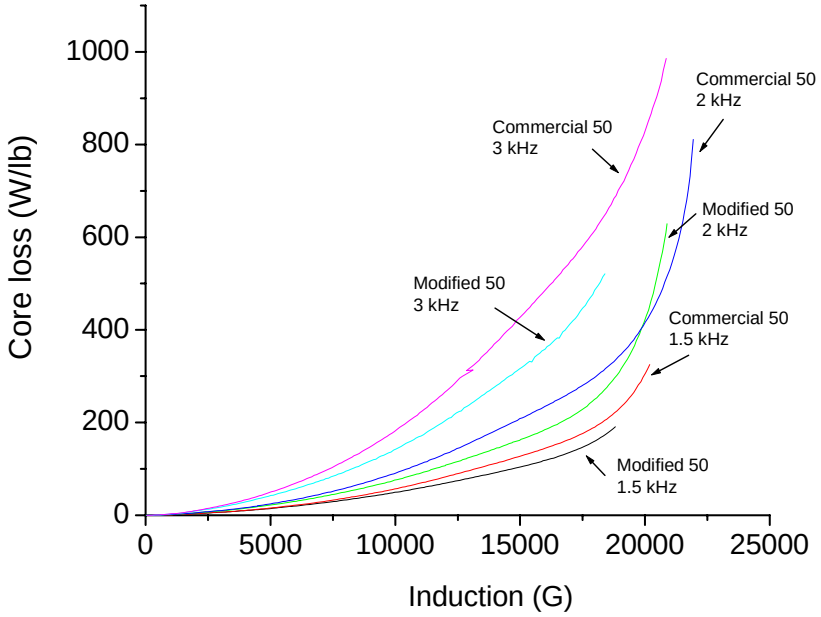

Figure 36. Core losses of modified Hiperco 50 and commercial Hiperco 50 at 1.5, 2, and 3 kHz.

The core losses of modified Hiperco 50HS and commercial Hiperco 50HS were also determined at various frequencies. Figure 37 shows the core losses of modified Hiperco 50HS and commercial Hiperco 50HS at 500 HZ and 3 kHz. It can be seen from Figure 37 that the modified Hiperco 50 HS has higher core losses than it commercial counterpart. As mentioned previously, because of the special composition of the Hiperco 50HS alloy, modifying commercial Hiperco 50HS by cold rolling and annealing actually does not significantly alter the grain size. Therefore, the core loss increase should be resulted from something other than grain size.

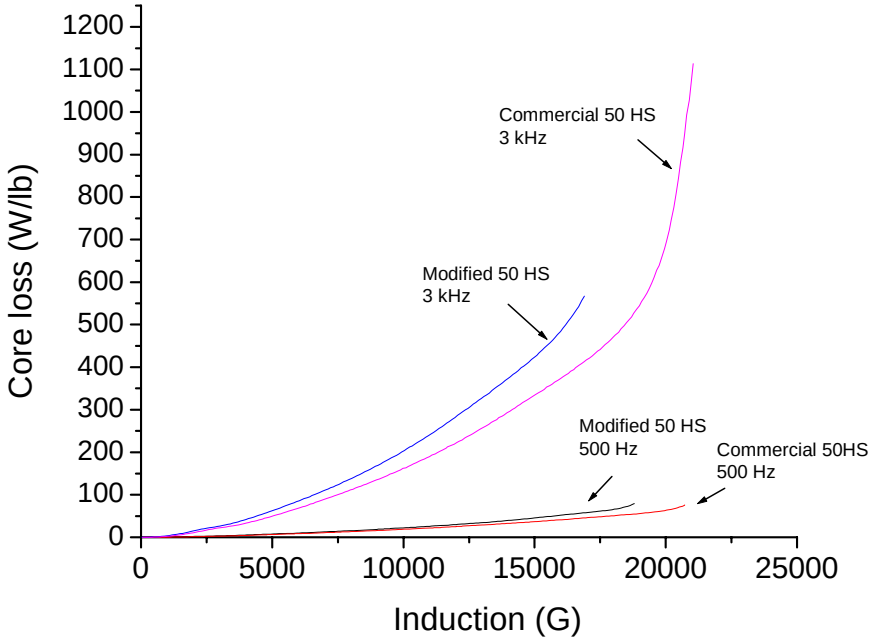

Figure 37. Core losses of modified Hiperco 50HS and commercial Hiperco 50HS at 500 HZ and 3 kHz.